Magnetotunneling in double-barrier heterostructures

A. Zaslavsky, D. C. Tsui, M. Santos, and M. Shayegan
Department of Electrical Engineering, Princeton University, Princeton, New Jersey 08544-5263
(Received 15 June 1989)

We report measurements of the current-voltage characteristics of an asymmetric $GaAs/Al_xGa_{1-x}As$ double-barrier resonant-tunneling device in a magnetic field **B** parallel to the tunneling direction. In the resonant-tunneling regime the magnetic field induces weak steplike features in the $I(V)$ curve and sawtooth oscillations in the $I(B)$ curve that are periodic in inverse field. We explain these magnetotunneling features by Landau quantization of the three-dimensional states in the emitter and the two-dimensional states in the well, which induces steplike structure in the tunneling supply function. The experimental $I(V,B)$ line shape is in good agreement with self-consistent numerical calculations.

Recent theoretical and experimental research into double-barrier resonant-tunneling structures (DBRTS) has advanced our understanding of charge transport in DBRTS.[1-4] The sequential-tunneling model of Luryi,[2] which invokes the conservation of energy and transverse momentum to determine the supply function of electrons that can tunnel elastically from the three-dimensional emitter into the two-dimensional well, has furnished a particularly clear explanation of the qualitative form of typical DBRTS I-V curves, wherein current begins to flow at a threshold bias V_{th}, increases nearly linearly in the resonant-tunneling regime between V_{th} and a peak voltage V_p, and then drops sharply. There have also appeared several studies of magnetotunneling effects in DBRTS, with the magnetic field **B** oriented either parallel[5-9] or perpendicular[10] to the tunneling direction [magnetotunneling studies have also been done in the silicon metal-oxide-semiconductor (MOS) system[11]]. In the first study of parallel-field magnetotunneling[5] it was pointed out that Landau quantization in the three-dimensional emitter should produce steps in the I-V curve, but uncertainty in the potential distribution over the device and the weakness of the field-induced features hindered comparison with the theory. In subsequent studies the magnetotunneling features were explained by the alignment of quantized two-dimensional Landau levels in the well and the emitter accumulation layer.[7,9] By conservation of transverse momentum this mechanism should produce sharp negative-differential-resistance (NDR) features in the tunneling regime, which have also been predicted by a numerical simulation of DBRTS magnetotunneling.[8] These features have not been observed experimentally, however.

In the course of studying the characteristics of asymmetric DBRTS, we have performed extensive magnetotunneling measurements in a parallel magnetic field. Instead of magnetically induced NDR features, we observe weak but unambiguous steps in the $I(V)$ curves of a high-quality DBRTS device at constant B and oscillations periodic in B^{-1} in $I(B)$ curves at constant V (similar to Shubnikov-de Haas oscillations). We explain these magnetotunneling features by extending the sequential tunneling model[2] to include a parallel magnetic field. This field quantizes the emitter density of states into Landau cylinders in momentum space,[12] whereas discrete Landau levels appear in the two-dimensional well. The conservation of energy and transverse momentum (or, equivalently, Landau-level index n) during tunneling leads to steplike structure in the supply function which, in turn, leads to the appearance of magnetotunneling features in the $I(V,B)$ characteristic of a DBRTS. Through a self-consistent calculation of the potential distribution over the device,[6] we have also calculated the $I(V,B)$ line shape of a DBRTS device in a parallel field and found very good agreement with the experimental data.

Our asymmetric DBRTS was grown by molecular beam epitaxy on an $n^+\langle 100\rangle$ GaAs substrate. The active region of our device consisted of (i) 0.5 μm of GaAs, Si doped to $\sim 2.2\times 10^{17}$ cm^{-3}, (ii) 50 Å of GaAs (spacer), (iii) 85 Å of $Al_{0.4}Ga_{0.6}As$ (lower barrier), (iv) 56 Å of GaAs (well), (v) 85 Å of $Al_{0.5}Ga_{0.5}As$ (higher barrier), (vi) 100 Å of GaAs (spacer), and (vii) 0.5 μm of $\sim 2.2\times 10^{17}$ cm^{-3} Si-doped GaAs. The barriers and the well were undoped, as were the spacer layers intended to prevent dopant diffusion into the barriers. The devices were defined by 10.5×10.5 μm^2 Au-Ni-Ge square dots, mesa-etched, and alloyed at 400 °C in hydrogen for Ohmic contacts.

All measurements were carried out at liquid-helium temperature with a computer-controlled voltage source stabilized by a small capacitor placed in parallel with and close to the device. The current was measured with a low-noise operational-amplifier circuit in order to eliminate the need for a current-sensing series resistor.

The zero-field $I(V)$ characteristic of our asymmetric DBRTS is shown in Fig. 1. It exhibits high peak to valley ratios in both forward- and reverse-bias polarities, the 29:1 ratio in the negative-bias polarity being a record for the $GaAs/Al_xGa_{1-x}As$ material system. Both bias polarities exhibit phonon-assisted tunneling features after the resonant peaks.[13] The asymmetry of the DBRTS

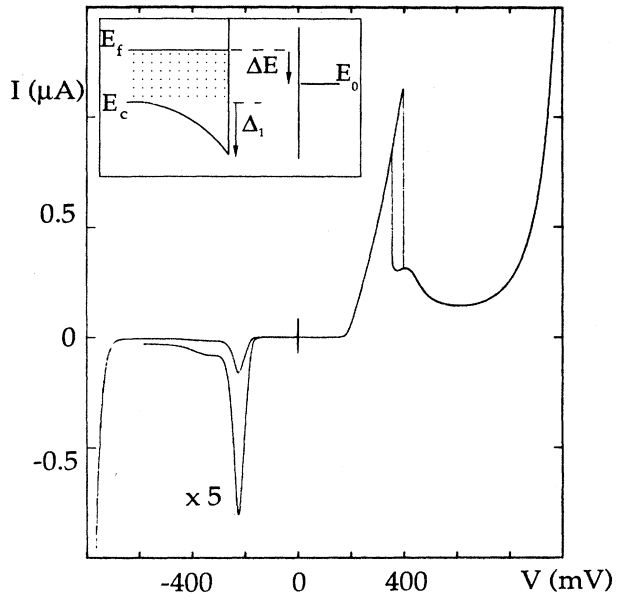

FIG. 1. I-V curve at $T=4.2$ K and zero magnetic field. Inset shows schematic band alignment in the tunneling regime, with ΔE defined as the energy separation between the resonant subband and E_F in the emitter.

design is reflected in the ratio of the peak currents in the two bias polarities of approximately 7:1 (in our convention forward bias refers to the polarity in which the emitter barrier is lower than the collector barrier). In addition, the asymmetric design maximizes the charge buildup in the well at forward bias and the $I(V)$ curve accordingly exhibits the intrinsic bistability which has been discussed elsewhere.[3,14,15] For this reason we have focused on the forward bias $I(V,B)$ characteristic of our device. In this report we shall concentrate on the forward-bias tunneling regime between $V_{\rm th}\approx 170$ mV and $V_p=400$ mV for tunneling through the first resonant subband. Our device also exhibits a second current peak at a higher forward bias $V=1.70$ V due to tunneling through the second subband, with a peak to valley ratio of better than 2:1 (not shown).

The magnetotunneling $I(V,B)$ data on our DBRTS are presented in Fig. 2. Figure 2(a) shows the $I(V)$ curves at constant B for three values of the magnetic field. The field induces weak steps in the $I(V)$ which grow stronger and move to higher bias at higher B values. The spacing between the steps increases proportionally with B, hence only one step is observed at $B=9.0$ and 7.0 T while two are observed at $B=5.0$ T [at still lower magnetic field values the steps become difficult to observe in the $I(V)$ but are clearly revealed in the conductance dI/dV, e.g., at $B=3.0$ T the $I(V)$ curve contains four steps].

In Fig. 2(b) we show $I(B)$ curves measured at constant V for three values of applied bias $V=325$, 350, and 375 mV. The $I(B)$ curves show clear oscillatory behavior, which becomes stronger at higher bias. Thus, at $V=375$ mV, which is fairly close to V_p, the oscillation amplitude $\Delta I/I$ reaches nearly 10% in the $B>5.0$ T range. The oscillations are periodic in B^{-1} and move to higher B values as the applied bias is increased. They also have a regular sawtooth shape which persists at all values of applied bias.

In order to explain these magnetotunneling features, we shall incorporate the presence of a parallel B into the sequential tunneling model—where electrons tunnel into the well elastically, conserving both energy and transverse momentum. Tunneling current begins to flow when the threshold applied bias $V_{\rm th}$ aligns the resonant subband E_0 with the emitter Fermi energy E_F. As more bias is applied the energy separation ΔE between the resonant subband E_0 and emitter E_F increases (see inset of Fig. 1), more electrons can tunnel elastically, and the current increases until E_0 lines up with the bottom of the conduc-

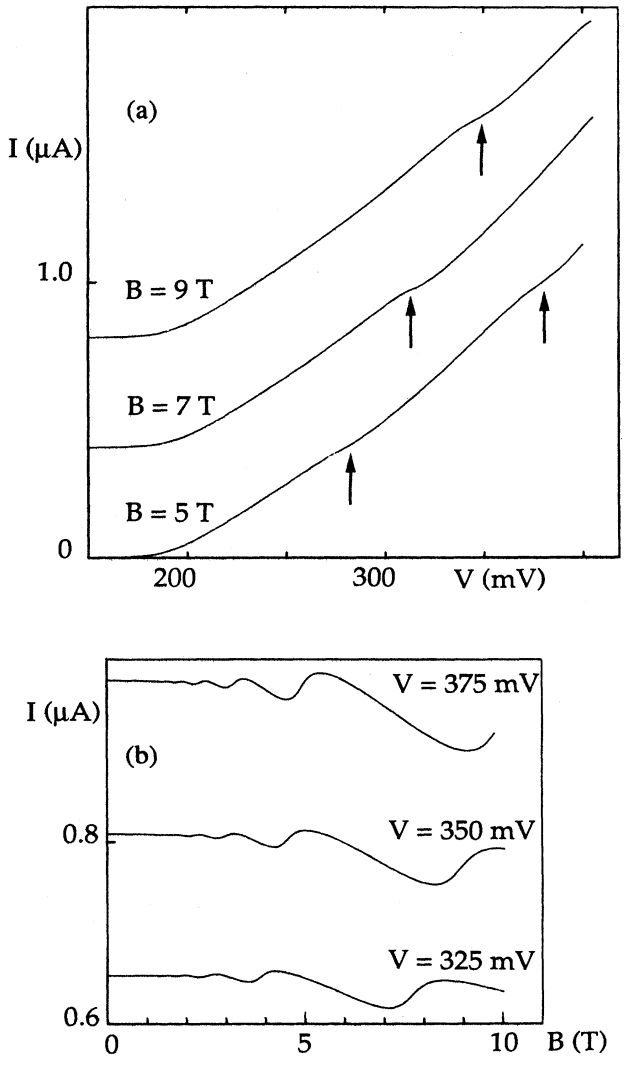

FIG. 2. (a) The forward bias $I(V)$ curves in the tunneling regime at parallel $B=5.0$, 7.0, and 9.0 T. The curves are displaced by 0.4 μA for clarity. Arrows mark the magnetic field-induced steps. (b) The forward bias $I(B)$ curves in the tunneling regime at total applied bias $V=325$, 350, and 375 mV.

tion band in the emitter (i.e., $\Delta E = E_F$) at V_p. A further increase in bias makes energy and transverse-momentum conserving tunneling impossible and the current drops sharply.

At $B=0$ the number of electronic states that can tunnel elastically from the three-dimensional emitter to the two-dimensional well, which we shall define as the supply function $N(\Delta E)$, can be easily estimated from the geometrical construction due to Luryi.[2] In an isotropic conduction band at low temperatures the electronic states of the emitter lie within a Fermi sphere in momentum space. Energy and transverse momentum conservation ensure that the electrons which can tunnel elastically lie on a constant $k_\parallel$ cross section through the Fermi sphere, where $k_\parallel$ is determined by the condition

$$E_\parallel = \hbar^2 k_\parallel^2 / 2m^* = E_F - \Delta E \ . \tag{1}$$

This situation is illustrated in Fig. 3(a). Since the energy width of the resonant subband is very small,[1] an estimate of the tunneling supply function is simply obtained by integrating over the tunneling states [i.e., the shaded disk in Fig. 3(a)]:

$$\begin{aligned} N(\Delta E) &= 2(2\pi)^{-3} \int\int \delta(k - k_\parallel(\Delta E)) dk_\parallel \, dk_\perp \\ &= (m^*/\pi\hbar^2) \int dE_\perp \\ &= (m^*/\pi\hbar^2) \Delta E \ , \end{aligned} \tag{2}$$

where $k_\parallel(\Delta E)$ is obtained from (1) and only $k_\parallel > 0$ states contribute. The total current from three-dimensional emitter states into the well has been derived earlier[3] as

$$J_1 \sim (e/2\pi\hbar) N(\Delta E) T_e (E_F + \Delta_1 - \Delta E) \ , \tag{3}$$

where T_e is the transmission coefficient of the emitter barrier (see also inset of Fig. 1). Although the potential distribution over the device and hence the quantities Δ_1, ΔE, and T_e must be calculated self-consistently with the total bias and current, we find that to first order the current is proportional to the tunneling supply function $N(\Delta E)$.

In a parallel magnetic field the electronic states in the three-dimensional emitter are quantized into Landau cylinders, as shown in Fig. 3(b). The conservation of energy and Landau index n (equivalent to transverse momentum) now makes the supply function depend on the number of Landau cylinders that pass through the constant $k_\parallel$ cross section of Eq. (1), rather than on the total area of this cross section. In the limiting case of infinitely sharp Landau quantization, the tunneling supply function reduces to a "staircase" shape: $N(\Delta E, B) = p(\Delta E, B) g(B)$, where $p(\Delta E, B)$ is the (integer) number of Landau cylinders passing through the constant $k_\parallel$ cross section [see Fig. 3(b)] and $g(B)$ is the Landau-level degeneracy. In a real DBRTS the Landau cylinders in the emitter (as well as the Landau circles in the two-dimensional well) are broadened by scattering, which smooths the supply function "staircase." In Fig. 3(c) we plot $N(\Delta E, B)$ of our device for $B=0$ and 5.0 T, where we have assumed Gaussian broadening of the emitter and well Landau levels, with a combined broadening of 2.5 meV.

It is worth noting, at this point, that the electronic states in the three-dimensional collector electrode are also quantized into Landau cylinders by the magnetic field. However, in the collector electrode the momentum component parallel to the direction of tunneling is unconstrained and the electric field in the depletion region sweeps the electrons away from the collector barrier. Consequently, any electron stored in the well always has an available empty collector state to tunnel into elastically, conserving both energy and the Landau-level index n. Hence the Landau quantization in the collector should not affect the measured $I(V)$ curve and, indeed, no quantization effects from the collector electrode are observed.

The geometrical construction of Fig. 3 provides an immediate qualitative explanation of the observed magnetotunneling features. As more bias is applied in the elastic tunneling regime the constant $k_\parallel$ cross section of electronic states that satisfy selection rule (1) is lowered through the emitter Landau cylinders, as shown in Fig. 3(b). But in a magnetic field the supply function is no longer strictly proportional to the area of the shaded disk, but rather reflects the Landau density of states structure, shown in Fig. 3(c) for the case of significantly broadened Landau levels. This structure, which appears as a series of smoothed steps, is observed in the $I(V)$

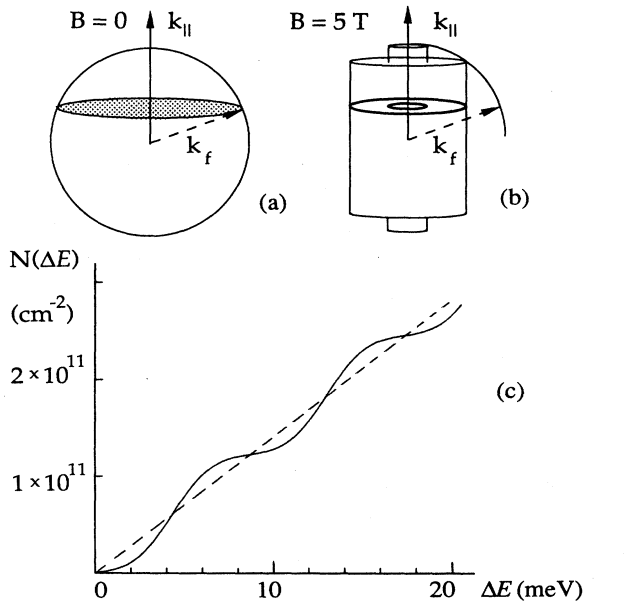

FIG. 3. The momentum space distribution of the electronic states in the three-dimensional emitter for (a) $B=0$ T and (b) $B=5.0$ T. The electrons which can tunnel elastically at some ΔE occupy the states in the shaded disc at $B=0$ T (a). At $B=5.0$ T these electronic states are compressed into rings (b). The corresponding supply functions $N(\Delta E)$ are plotted for $B=0$ T (dashed line) and $B=5.0$ T (solid line) in (c). The $B=5.0$ T supply function was calculated by assuming the emitter Landau cylinders to be Gaussian in energy with 2.5 meV broadening.

curve. The steps in the supply function occur at integral multiples of $\hbar\omega_c$, where ω_c is the cyclotron frequency. For our doping of $\sim 2.2\times 10^{17}$ cm^{-3}, we have a Fermi level of ~ 20 meV, and hence observe two steps at $B=5.0$ T ($\hbar\omega_c=8.6$ meV), but only one step at $B=7.0$ T ($\hbar\omega_c=12.1$ meV). We note that this method can yield an accurate estimate of the actual doping in the DBRTS electrodes.

When $I(B)$ is measured at constant applied bias and a ramped B field, the Landau cylinders in Fig. 3(b) expand and gradually leave the Fermi sphere. To first order, ΔE and hence the position of the shaded disk in Fig. 3(b) remain unchanged [ignoring the self-consistent feedback of the oscillating current in Fig. 2(b) on the potential distribution across the device]. The situation is then analogous to the normal Shubnikov–de Haas oscillations: as the Landau cylinders escape from the constant $k_\parallel$ cross section of the Fermi sphere, defined by selection rule (1), the tunneling supply function oscillates periodically in B^{-1}. The corresponding current oscillations are shown in the data in Fig. 2(b). Here it should be noted that the Fermi energy in the emitter also oscillates as a function of B.[11]

In order to further understand the magnetotunneling features, we have performed a self-consistent numerical calculation of the $I(V)$ curve of our DBRTS with and without a parallel magnetic field. The self-consistent potential distribution over the device, taking into account the accumulation and depletion layers outside the emitter and collector barriers, respectively, as well as the charge density σ_w dynamically stored in the well, was calculated from the self-consistent system of equations in Ref. 6. The transmission coefficients of the barriers were calculated in the WKB approximation. Although excellent quantitative agreement with experimental data can be obtained by using the electron mass in the barrier as a fitting parameter,[16] we chose the usual nonparabolic expression for the mass of an electron with energy E:[17]

$$m^*(E)\approx m^*_{\rm CB}(1+2E/E_g)\ , \tag{4}$$

where $m^*_{\rm CB}$ is the conduction-band-edge mass and E_g is the band gap. The current into the well J_1 is then given by Eq. (3) multiplied by the additional factor

$$\gamma(\Delta E,\sigma_w)=\frac{(m^*\Delta E/\pi\hbar^2)-(\sigma_w/e)}{(m^*\Delta E/\pi\hbar^2)} \tag{5}$$

which determines the fraction of states in the well that is unoccupied by the dynamically stored charge and thus available for elastic tunneling. The current out of the well J_2 is given by[6]

$$J_2=\sigma_w E_0 T_c/\hbar\ . \tag{6}$$

In steady state the currents into and out of the well must be equal, i.e., $J_1=J_2$, which closes the self-consistent system of equations and permits one to calculate the expected $I(V)$ curve of the device given the DBRTS material parameters—electrode doping, the height and width of the barriers, and the extent of the spacer layers.

The presence of the magnetic field affects the calculation through the structure that appears in the tunneling supply function as discussed above. The use of the WKB approximation in the expressions for the tunneling current, with electron mass given by (4), yields current densities that are nearly an order of magnitude too large,[7] but, once the calculated peak current is normalized to the experimentally measured value, the agreement between the calculated and experimental I-V line shapes is very good. The calculated $I(V)$ curve at zero temperature, $B=5.0$ T, Landau-level broadening of 1.5 meV, electrode doping of 2.3×10^{17} cm^{-3}, barriers of 320 and 433 meV, and collector spacer layer of 70 Å is compared to the experimental data in Fig. 4. The abrupt turn on of the tunneling current in the calculated $I(V)$ curve is due to the assumption of zero temperature and neglect of band tailing in the calculation. We note that while the calculated current densities are strongly dependent on the effective mass of the tunneling electrons and the precise height and width of the $Al_xGa_{1-x}As$ barriers, the normalized $I(V,B)$ line shape is much less sensitive to these parameters.

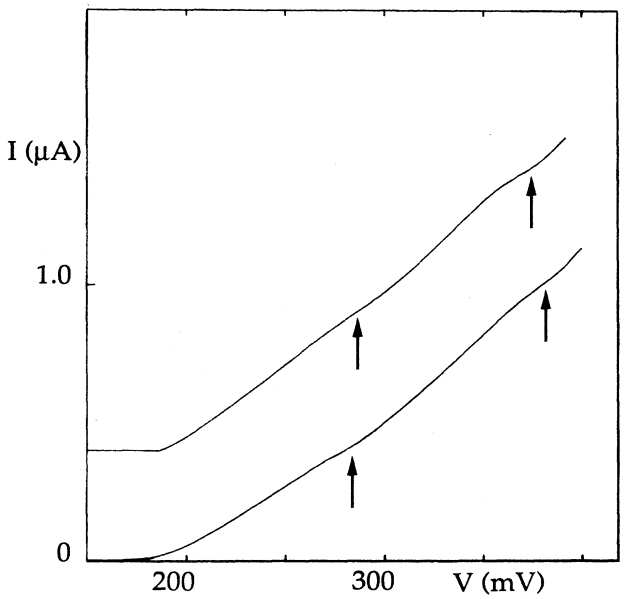

FIG. 4. Measured (lower curve) and calculated (upper curve) $I(V)$ line shapes at $B=5.0$ T (the calculated curve is normalized to the measured peak current). The line shapes are displaced 0.4 μA for clarity. Arrows mark the field-induced steps. The calculation parameters are listed in the text.

In conclusion, we have measured the current-voltage characteristics of a high-quality, asymmetric DBRTS device in a parallel magnetic field **B**. We observed unambiguous, although weak, steplike features in the $I(V)$ curve at constant B and oscillations periodic in B^{-1} in the $I(B)$ curve at constant V. The steps in the $I(V)$ curve are a signature of magnetotunneling from a three-dimensional to a two-dimensional density of states. We have interpreted our data by extending the sequential tunneling model to the case of a parallel magnetic field. Our numerical simulation of the $I(V,B)$ line shape of the device is in very good agreement with the experimental data.

ACKNOWLEDGMENTS

The authors gratefully acknowledge a fruitful discussion with Professor V. J. Goldman and technical assistance by Y. Li and T. Sajoto. This work has been supported by the U.S. Army Research Office under Contract No. DAAL03-89-K-0036 and by the U.S. National Science Foundation under Grant No. ECS-85-53110. A. Z. acknowledges partial support by IBM.

[1]B. Weil and T. Vinter, Appl. Phys. Lett. **50**, 1281 (1987); M. Jonson and A. Grincwajg, Appl. Phys. Lett. **51**, 1729 (1987).

[2]S. Luryi, Appl. Phys. Lett. **47**, 490 (1985).

[3]V. J. Goldman, D. C. Tsui, and J. E. Cunningham, Phys. Rev. Lett. **58**, 1256 (1987).

[4]J. F. Young, B. M. Wood, G. C. Aers, R. L. S. Devine, H. C. Liu, D. Landheer, M. Buchanan, J. SpringThorpe, and P. Mandeville, Phys. Rev. Lett. **60**, 2085 (1988).

[5]E. E. Mendez, L. Esaki, and W. I. Wang, Phys. Rev. B **33**, 2893 (1986).

[6]V. J. Goldman, D. C. Tsui, and J. E. Cunningham, Phys. Rev. B **35**, 9387 (1987).

[7]M. L. Leadbeater, E. S. Alves, L. Eaves, M. Henini, O. H. Hughes, A. Celeste, J. C. Portal, G. Hill, and A. Pate, Phys. Rev. B **39**, 3438 (1989).

[8]C. E. T. Gonçalves da Silva and E. E. Mendez, Phys. Rev. B **38**, 3994 (1988).

[9]S. Ben Amor, K. P. Martin, J. J. L. Rascol, R. J. Higgins, R. C. Potter, A. A. Lakhani, and H. Hier, Appl. Phys. Lett. **54**, 1908 (1989).

[10]P. England, J. R. Hayes, M. Helm, J. P. Harbison, L. T. Florez, and S. J. Allen, Jr., Appl. Phys. Lett. **54**, 1469 (1989); M. Helm, F. M. Peeters, P. England, J. R. Hayes, and E. Colas, Phys. Rev. B **39**, 3427 (1989).

[11]A. Hartstein and R. H. Koch, Phys. Rev. B **35**, 6442 (1987).

[12]K. Seeger, *Semiconductor Physics* (Springer-Verlag, New York, 1985).

[13]V. J. Goldman, D. C. Tsui, and J. E. Cunningham, Phys. Rev. B **36**, 7635 (1987).

[14]F. Sheard and J. C. Toombs, Appl. Phys. Lett. **52**, 1228 (1988).

[15]A. Zaslavsky, V. J. Goldman, D. C. Tsui, and J. E. Cunningham, Appl. Phys. Lett. **53**, 1408 (1988).

[16]S. Kurtin, T. C. McGill, and C. A. Mead, Phys. Rev. Lett. **25**, 756 (1970).

[17]C. K. Williams, T. H. Glisson, M. A. Littlejohn, and J. R. Hauser, IEEE Electron. Dev. Lett. **EDL-4**, 161 (1983).